Electrodeposition of Indium Antimonide Nanowires in Porous Anodic Alumina Membranes

Asaduzzaman Mohammad[1], Suprem R. Das[2], Yong P. Chen[2,1], Timothy D. Sands[1, 3], and David B. Janes[1,]*

1. *School of Electrical and Computer Engineering and Birck Nanotechnology Center, Purdue University, West Lafayette, IN 47907, USA*
2. *Department of Physics and Birck Nanotechnology Center, Purdue University, West Lafayette, IN 47907, USA*
3. *School of Materials Engineering and Birck Nanotechnology Center, Purdue University, West Lafayette, IN 47907, USA*

Abstract - Vertical arrays of high aspect ratio (>100) InSb nanowires with diameters of ~20 nm have been fabricated using a Porous Anodic Alumina (PAA) template that is supported on a Si substrate with a thin layer of titanium (Ti) sandwiched between them. The process described here uses a reverse anodization technique to penetrate the hemispherical pore bottom barrier oxide layer prior to the electrodeposition process, so as to form a direct electrical contact with the underlying Ti layer. Scanning electron microscopy results demonstrate that the InSb nanowires completely fill the channels of the PAA thereby acquiring a wire diameter of about 20 nm. Raman spectrum of the InSb nanowires indicates high crystal quality.

Keywords- Porous Anodic Alumina (PAA); Anodization, Electrodeposition, Nanowires, Indium Antimonide (InSb)

I. INTRODUCTION

Indium Antimonide (InSb) has gained a significant amount of interest and recognition for many of its intrinsic qualities. It is a III-V semiconductor with its bulk form displaying a narrow direct band gap of about 0.18 eV, very high electron mobility (μ_e ~ 80000 cm^2/Vs) and is known to have ballistic lengths of up to 700 nm (at 300K). These qualities of InSb make it a potential candidate for infrared detection arrays, high speed electronics and magnetoresistive sensors [1,3,12]. Furthermore InSb nanowires are known to exhibit quantum confinement effects and one dimensionality when the wire diameter is less than 23 nm. In this work high aspect ratio (>100) InSb nanowires with an average diameter of around 15-20 nm have been synthesized.

With the increase in interest in nanowire device research, the efficient fabrication of uniform nanowires on templates has become an active area of research [1-3, 5]. There have been various studies that have proven the usefulness of nanowires in various applications in sensors [1] to thermoelectrics [4] to transistors [3]. The ability to control the pore diameter and aspect ratio of the self-organized 'nanopore' structures of PAA membranes make them a convenient template for the synthesis of nanowires arrays [3, 5-8]. In this work, the PAA template is fabricated by anodizing a 1.5 µm layer of Al deposited over a 100 nm layer of titanium (Ti) on a Si wafer with. It is extremely difficult to handle free standing PAA templates of less than 10 µm thickness due to their fragility. Therefore in this study the PAA is fabricated on top of a Si wafer to provide a structural stability to the template and make it suitable for device fabrication. The Ti layer serves as an adhesion layer and an auxiliary conductive path during the subsequent electrodeposition process. One of the greatest challenges in using a PAA template is the presence of a hemispherical pore bottom oxide barrier layer, which can hinder the creation of an electrical contact at the bottom of the pores. There are various methods that have been used to break through the pore bottom barrier oxide layer including chemical or plasma etching processes [5, 9], but these processes introduce a pore widening effect that can negatively impact the aspect ratios of the wires. In this study, the pore bottoms have been penetrated using a reverse bias anodization technique, which has been performed in situ without any noticeable expansion in the pore diameters.

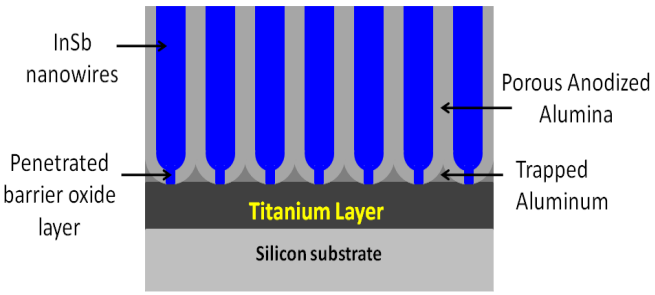

Fig. 1 Schematic view of InSb nanowires inside the pores of PAA template.

There have been various methods that have been used to fabricate nanowires that include the vapor deposition and vapor-liquid-solid (VLS) methods. Due to 'pore closure' effects, it is difficult to achieve high aspect ratio nanowires (greater than 100 in the PAA template) using vapor deposition. On the other hand, the growth of nanowires using the VLS method may introduce non-uniformity in the nanowires. In this work, an electrodeposition process has been employed to deposit the InSb nanowires within the pores in the PAA. Figure 1 shows a schematic view of the InSb nanowires deposited inside the channels of a PAA template.

II. EXPERIMENTAL PROCEDURES

Synthesis of the PAA Templates

A thin layer of titanium (100nm), followed by a layer of aluminum (1.5 µm), was deposited on a thermally oxidized silicon substrate using an electron-beam evaporator with a

US 978-1-4244-4732-9/10/$25.00 ©2010 IEEE

base pressure of 0.5 to 1×10^{-6} torr. In addition to acting as an adhesion layer, the Ti layer serves as the back electrode for anodization and electrodeposition. The Al deposited sample was then rinsed with DI water, acetone and methanol in order to remove any residual organic impurities from the surface of the samples. Since H_2SO_4 solutions are known to yield the smallest pore diameters, the deposited Al layer was anodized in a 0.3M H_2SO_4 (sulfuric acid) solution at an anodization voltage of 20V [5, 9] and a constant temperature of 4ºC.

In order to improve the ordering of the nano pores in the PAA template, a two-step anodization process has been used [5, 9]. After anodizing a portion of the Al layer during the first step of anodization, the PAA membrane was stripped off by using a heated mixture of diluted chromic and phosphoric acids. This would cause the formation of fairly regular dimples on the resurfaced Al layer left behind by the hemispherical pore bottoms of the first step of anodization. These dimples or depressions would serve as the initiation sites for the second anodization step. The second anodization is run until the Al_2O_3 pore membrane reaches the Ti layer.

Penetration of the Pore Bottom Oxide Barrier Layer

The formation of the insulating barrier oxide layer at the pore bottom is an inherent property of PAA that is regularly seen when anodizing Al. The breakthrough of the barrier layer is absolutely crucial for the electrodeposition process. The opening in the barrier layer would expose the underlying Ti layer that would act as one of the electrodes during the electrodeposition process. A reverse bias anodization technique has been used to penetrate the pore bottom oxide barrier layer [6, 7]. This process is initiated immediately after the anodization process by applying a reverse bias voltage of -3.5V to the PAA template in the same electrolytic set-up and environment. The process causes the evolution of hydrogen bubbles from the surface of the PAA template once the hydrogen ion penetrates the pore bottom oxide layer and reduces on the exposed Ti layer (cathode). The reverse bias anodization procedure was applied for five minutes before bringing down the magnitude of the applied voltage to zero. Although on penetration of the pore bottom oxide layer, the 0.3M H_2SO_4 electrolyte is dilute enough to not oxidize the underlying Ti layer by forming columnar structures; care was taken not to permit the formation of large voids at the Ti/PAA interface. This was done by mathematically estimating the time required to penetrate the 20 nm (approx.) thick pore bottom oxide barrier layer. In case large voids do form at the Ti/PAA interface, there is a high possibility for the PAA template to lift-off from the silicon substrate. This is caused by the added tensile pressure of H_2 gas at the PAA/Ti interface on top of the pre-existing stress the sample experiences due to the volume expansion during the anodization of Al to form PAA.

Electrodeposition of the InSb nanowires

The penetrated pore bottom PAA membranes were then used as the templates into which the InSb nanowires were electrodeposited. The electrodeposition process was conducted in a three electrode electrochemical cell with the PAA template as the working electrode, platinum electrode as the counter electrode and Ag/AgCl as the reference electrode. The entire electrodeposition process was controlled and carried out by a potentiostat/galvanostat (Princeton Applied Research, model: Potentiostat 263A). The deposition parameters used for the experiment are as follows: 0.1M $SbCl_3$, 0.15M $InCl_3$, 0.36M citric acid, and 0.17M potassium citrate. The citrate ions have been used as complexing agents that bring the deposition potential of In and Sb closer to maintain a binary growth during the deposition of the InSb nanowires [2, 8]. The deposition was conducted for 45 minutes at a potential of -0.85V to -1.5V versus the reference electrode (Ag/AgCl) at room temperature. On completion of the deposition process the PAA template was rinsed with DI water.

III. CHARACTERIZATION

The structural and material properties of the InSb nanowires were analyzed by Raman Spectroscopy imaging and Field Effect Scanning Electron Microscope (FESEM) imaging. The synthesized InSb nanowires were observed by using a FESEM (Hitachi S-4800) by looking at the cross-section and the surface of the PAA template. The Raman spectra of the InSb nanowires were taken at room temperature using different laser powers at room temperature, using an excitation source with a wavelength (λ) of 532 nm in a backscattered geometry.

IV. RESULTS AND DISCUSSIONS

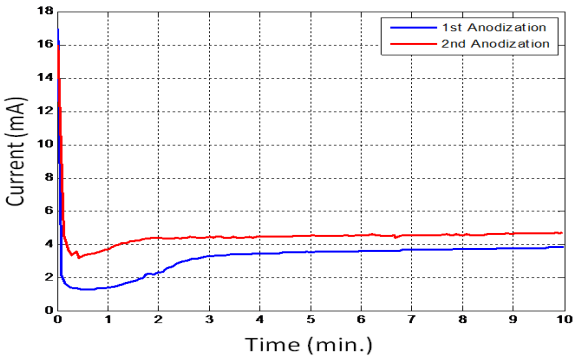

Fig. 2 Anodization current vs. time for the first and second step of Al anodization

Fig. 2 shows the current vs. time data obtained during the formation of the PAA template for the first and second step anodization. The first anodization process, which left behind the depressions, results in a lower oxide resistance during the second anodization process and thereby a slight increase in the current flow was observed.

At the final stages of anodization, the current drops dramatically signaling the consumption of the entire Al layer to form the PAA membrane as shown in Fig. 3. The fabricated PAA templates display pore density in the order of ~10^{10} pores/cm^2, with the average diameter of around 20 nm and

aspect ratio of greater than 100. The FESEM image of the cross-section of the PAA template displayed parallel porous structures, as seen in Fig. 4

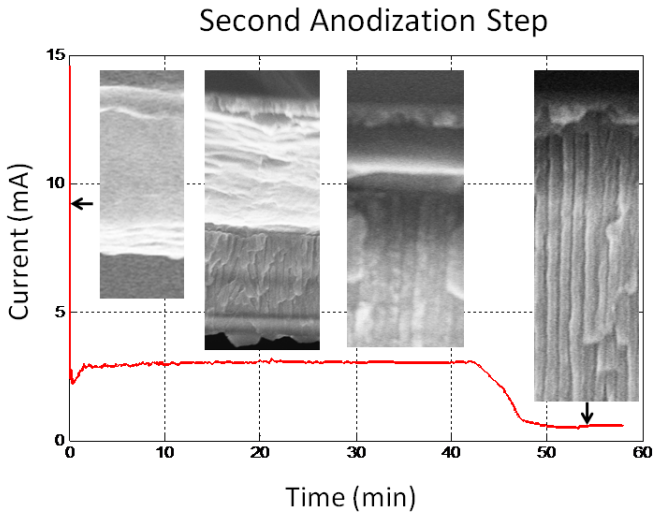

Fig. 3. Anodization current vs. time for second step anodization. Insets show various stages of PAA formation.

.

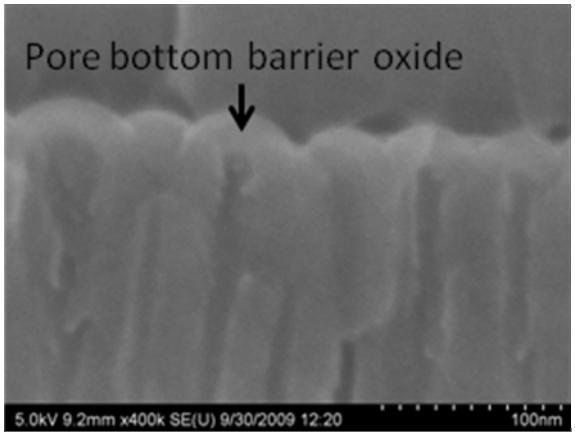

Fig. 4. FESEM image showing the average pore diameter and the hemispherical pore bottom

Fig. 5 shows the penetration of the oxide barrier layers at the pore bottoms by a reverse anodization immediately after the formation of PAA. This process leads to the concentration of the H^+ ions (from the electrolyte) at the pore bottoms where the electric field is most concentrated. During the reverse anodization process the H^+ ions dissolve the oxide barrier layer and on penetration of the oxide layer it gets reduced on the underlying Ti layer (cathode) [7]. The entire reaction may be summarized as follows:

$Al_2O_3 + 6H^+ \rightarrow 2Al^{3+} + 3\ H_2O$ (during the dissolution of the oxide layer)
$2H^+ + 2\ e^- \rightarrow H_2$ (once the penetration is completed)

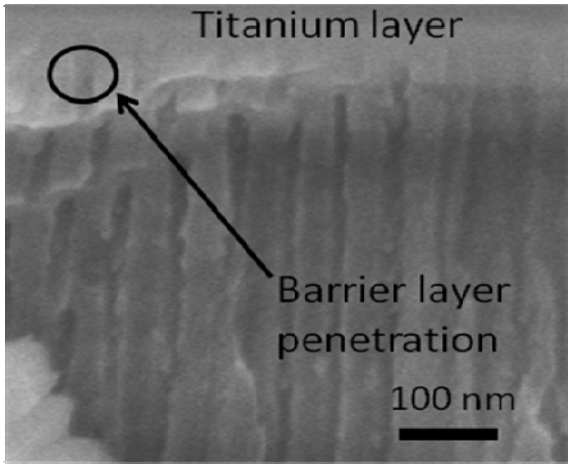

Fig. 5. FESEM image showing the barrier layer penetration of the pore bottoms

During the electrodeposition process the deposition current was closely monitored. Fig. 6 depicts the deposition current vs. time graph of the InSb nanowires inside the nanochannels of the PAA template. During the first few seconds of the deposition process the current is observed to be relatively small due to the initial deposition of InSb on the Ti layer, which acts as the seed for the subsequent nanowire growth. The steady increase in current with the growth of the nanowires is believed to be due to an increased diffusion of ions to the nanowire growth front.

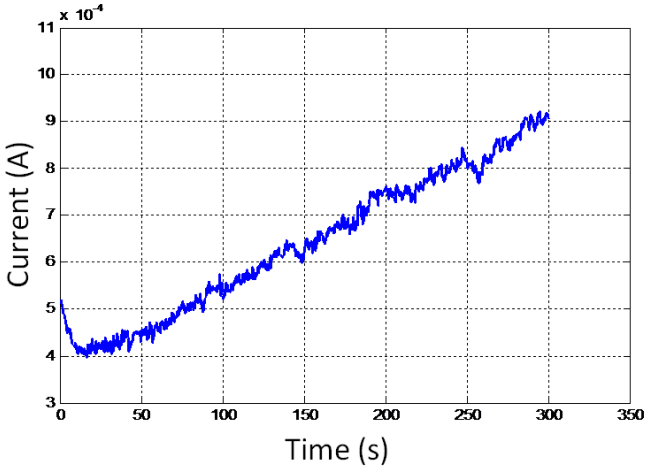

Fig. 6. Current vs. time graph for InSb nanowire deposition during the first few minutes.

The synthesized InSb nanowires (Fig. 7 shows the FESEM images of the wires) appear to fill up the pore channels, demonstrating similar aspect ratios (>100) and diameters as that of the actual pores (~20 nm). The fill factor of the PAA templates has been observed to be around 10-20%. The fill factor may be increased if the wettability of the PAA template can be increased, which is a challenge due to the extremely small sizes of the pores.

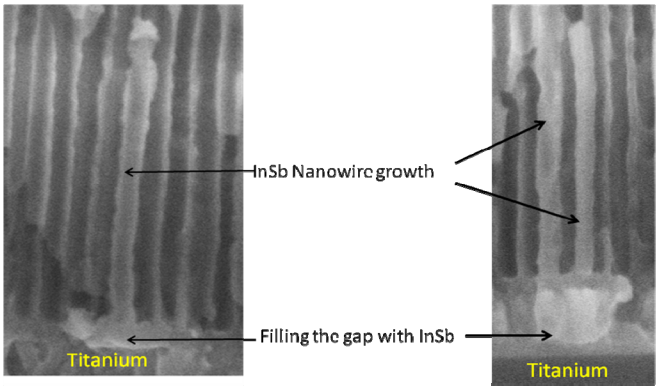

Fig. 7. FESEM images of InSb nanowires grown along the length of the pores.

Fig. 8 a-b show the Raman spectra of the InSb nanowires captured in a backscattered geometry using 532nm laser excitation source at room temperature. The Raman spectra reveal the distinct peaks of the TO and LO phonon modes of the InSb nanowires at 178 cm^{-1} and 192 cm^{-1} respectively deposited at a potential of -1.5V and at 179 cm^{-1} (TO) and 190 cm^{-1} (LO) for the wires deposited at a potential of -1.0V. The TO and LO phonon modes of the deposited wires match closely with the TO and LO peaks of bulk InSb and prior InSb nanowires studies [2, 10-11]. Furthermore, the clear splitting and formation of distinct peaks for the TO and LO modes of phonon vibration in the sample indicates the formation of well crystallized InSb nanowires.

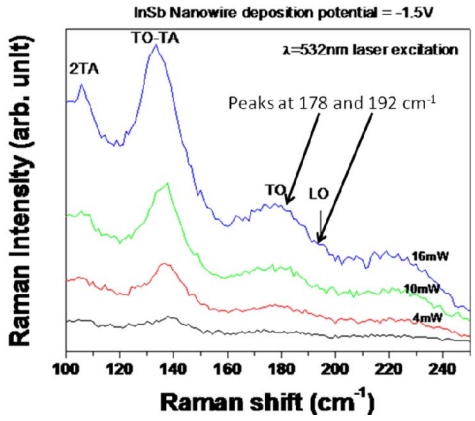

Fig. 8a. Raman spectra of InSb nanowires deposited at -1.5 V

V. CONCLUSIONS

In summary the PAA template was fabricated in a sulfuric acid solution so as to get pores with diameters in the range of 15-20 nm. The pore bottom oxide barrier layer of the PAA template has been successfully penetrated by applying a reverse bias anodization technique. In the end well crystallized InSb nanowires have been synthesized by using dc electrodeposition inside the channels of the fabricated PAA template. The InSb nanowires have been observed to fill up the channels of the PAA template and therefore exhibit wire diameters of about 20 nm, which would make these 1D nanowires and therefore have potential applications in infrared optical detectors and high speed electronic devices.

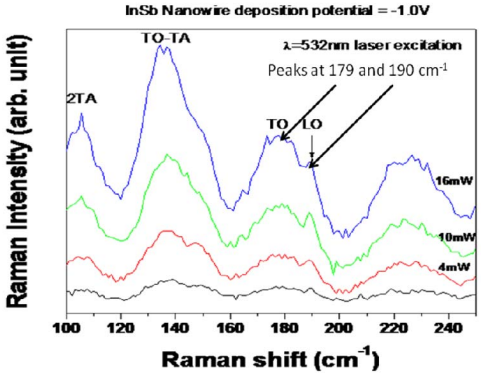

Fig. 8b. Raman spectra of InSb nanowires deposited at -1.0V.

REFERENCES

[1] H. Chen, X. Sun, K. W. C. Lai, M. Meyyappan, and N. Xi, "Infrared Detection using an InSb nanowire", IEEE Nanotechnology Materials and Devices Conference (2009).

[2] X. Zhang, Y. Hao, G. Meng, L. Zhang, "Fabrication of highly ordered InSb Nanowire arrays by electrodeposition in porous anodic alumina membranes", J. Electrochem. Soc., 2005, C664-668.

[3] X. Jing, M. Penchev, J. Zhong, R. Paul, M. Ozkan, C. Ozkan, "InSb nanowires based field effect transistor", Proc. Of SPIE,2009, Vol. 7402.

[4] N. Mingo, "Thermoelectric figure of merit and maximum power factor in III-V semiconductor nanowires", Appl. Phys. Lett. 84, 2652, (2004).

[5] A. D. Franklin, M. R. Maschmann, M. DaSilva, D. B. Janes, T. S. Fisher, T. D. Sands, "In-place fabrication of nanowire electrode arrays for vertical nanoelectronics on Si substrates", J. Vac. Sci. Technol., Mar/Apr 2007, 343-347.

[6] O. Rabin, P. R. Herz, Y. M. Lin, A. I. Akinwande, S. B. Kronin, M. S. Dresselhaus, "Formation of a thick porous anodic alumina films and nanowires arrays on silicon wafer and glass.", Adv. Func. Mat.2003; 13, 631-8.

[7] M. Tian, S. Xu, J. Wang, N. Kumar, E. Wertz, Q. Li, P. M. Campbell, M. H. W. Chan, and T. E. Mallouk, "Penetrating the Oxide Barrier in situ and Separating Freestanding Porous Anodic Alumina Films in One Step", Nano Lett., 2005, Vol. 5, No. 4, 697-703.

[8] M. I. Khan, X. Wang, K. N. Bozhilov, C. S. Ozkan, "Templated Fabrication of InSb Nnaowires for Nanoelectronics", J. Nanomaterials, vol. 2008, Article ID 698759.

[9] Y. Lei, W. Cai, G. Wilde, "Highly ordered nanostructures with tunable size, shape and properties: A new way to surface nano-patterning using ultra-thin alumina masks", Progress in Materials Science, 52 (2007) 465-539

[10] A. Pinczuk, and E. Burstein, "Raman Scattering from InSb surfaces at photon energies near the E_1 energy gap", Phys. Rev. Lett., 1968, vol 21, 1073-1075.

[11] V. Wagner, D. Drews, N. Esser, D. R. T. Zahn, J. Geurts, W. Richter, "Raman monitoring of semiconductor growth", J. Appl. Phys., 1994, 7330-7333.

[12] S. A. Solin, T. Thio, D. R. Hines, J. J. Heremans, "Enhanced Room-Temperature Geometric Magnetoresistance in Inhomogeneous Narrow-Gap Semiconductors", Science 289, 1530, (2000).